μ-Synthesis Control for a Walking Robot

Satinder Pannu, H. Kazerooni, Gregory Becker, and Andrew Packard

Developing a two-legged walking robot has been the topic of research for many years now. Many of the walking machines developed so far have large feet in order to allow substantial torque to be generated by motors located at the ankles. One approach to avoid this problem is to balance the system with only actuation at the knee and leave the ankle unactuated.

An experimental system built at the University of California at Berkeley (Fig. 1) provides insight into the design and control of a machine that must stand on its own. This experimental machine has two links which are powered relative to each other by a DC motor at Joint 2 (i.e., the knee). Joint 1 (i.e., the ankle) at ground level is not powered: a motor at Joint 1 would require a prohibitively large and lengthy foot similar to a snow ski. Because the ankle joint has no actuation, the machine remains upright only when it is balanced via a computer-controller. We show that the stability of such a machine can be accomplished using a single powered joint at the knee to adjust the center of mass. In other words, the controller must keep the machine's center of mass directly above the machine's ankles for stability. For a two-legged walking machine, we propose using two legs with the aforementioned property: no actuation at the ankle [1].

The stabilizing controller for the walking robot uses only one leg of the system; the remaining leg follows a command for locomotion. Suppose the left leg (labeled "L" in Fig. 2) is using the left knee actuator to stabilize the system. Then the right leg (labeled "R" in Fig. 2) is under the computer control and moves autonomously in an unconstrained space (a and b in Fig. 2) to produce locomotion of the system1. The left leg continues to stabilize the system until the right leg moves forward and contacts the ground (c). At this time a transition occurs, and stabilization is assigned to the right leg (d). The left leg no longer stabilizes and instead is now under the computer control (or human control in the exoskeleton case) for maneuvering in unconstrained space.

A walking machine has been designed and built at UC Berkeley, but the above theory for walking has not been experimentally verified yet. This article investigates designing a stabilizing controller using the μ-synthesis approach for one leg of the walking robot.

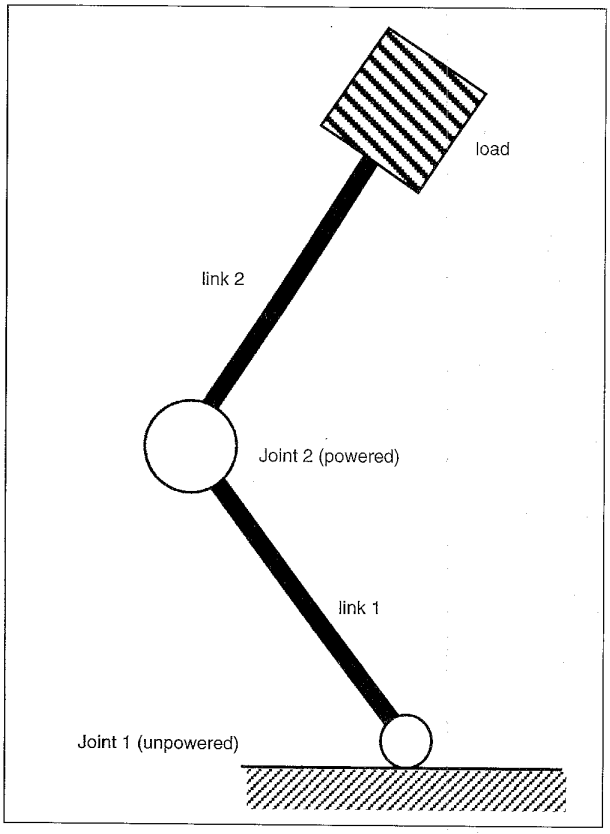

Fig. 1. An experimental under-actuated leg consisting of two links. Only Joint 2 is powered. Joint 1 is not powered and is in contact with the ground. The actuator at Joint 2 must be controlled in such a way that the center of mass of the entire system passes through Joint 1.

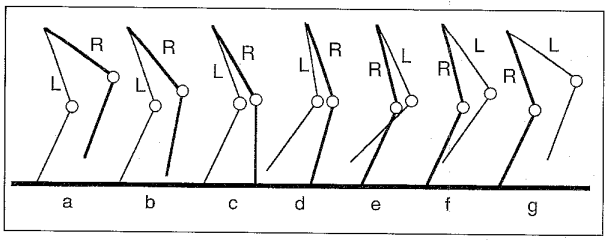

Fig. 2. The walking machine always stabilizes only on one leg while the other leg is under the computer control. This control technique allows for forward and backward motion.

[1]An exoskeleton [2,3] is being designed at UC Berkeley. Note that the right leg will be under the human operator's control (using a set of force sensors) and moves with the operator's leg (a and b in Fig. 2) to produce locomotion if the legs are a part of an exoskeleton system.

Correspondents please contact Professor H. Kazerooni, Mechanical Engineering Department, University of California, Berkeley, CA 94720-1740. *A version of this article was presented at IEEE International Conference on Robotics and Automation, Nagoya, Japan, May 21-27, 1995.*

0272-1708/96/$05.00©1996IEEE

Model

Fig. 3 shows the schematic used to model an under-actuated leg. It consists of two rigid links connected by a rotary joint. Link 1 is pivoted at the base so as to allow rotary motion but no translational motion. There is no actuation at this pivot point. A DC motor housed in Link 1 supplies torque to the rotary joint connecting Link 1 and Link 2. The torque is transferred from the motor to the transmission by a belt-and-pulley system. There are two degrees of freedom θ_1 and θ_2, of which only one is powered (θ_2). (See appendix for nomenclature.) Thus there is one less actuator than degrees of freedom. Such systems are called under-actuated.

The dynamic equations of motion, in the absence of any frictional forces, are

$$H\ddot{\theta} + V + G = \tau \tag{1}$$

where:

$$H_{11}(\theta_2) = I_1 + I_2 + M_1\left(L_{c1x}^2 + L_{c1x}^2\right) + M_2\left(L_1^2 + L_{c2}^2 + 2L_{c1y}L_{c2}\cos(\theta_2)\right)$$

$$H_{12}(\theta_2) = I_2 + M_2\left(L_{c2}^2 + L_1 L_{c2}\cos(\theta_2)\right)$$

$$H_{21}(\theta_2) = H_{12}$$

$$H_{22} = I_2 + n^2 I_m + M_2 L_{c2}^2$$

$$V_1 = -2M_2 L_1 L_{c2}\sin(\theta_2)\dot{\theta}_2\dot{\theta}_1 - M_2 L_1 L_{c2}\sin(\theta_2)\dot{\theta}_2^2$$

$$V_2 = M_2 L_1 L_{c2}\sin(\theta_2)\dot{\theta}_1^2$$

$$G_1 = M_1 g\left[L_{c1y}\cos(\theta_1) + L_{c1x}\sin(\theta_1)\right] + M_2 g\left[L_1\cos(\theta_1) + L_{c2}\cos(\theta_1 + \theta_2)\right]$$

$$G_2 = M_2 g L_{c2}\cos(\theta_1 + \theta_2)$$

$$\tau_1 = 0,\ \tau_2 = T$$

It is desired to control the system about an operating point where the center of mass of the system is above the pivot point. Equilibrium is defined as configuration where $\ddot{\theta}_1 = \ddot{\theta}_2 = \dot{\theta}_1 = \dot{\theta}_2 = 0$ in Equation 1, which leads to

$$\cos(\theta_{1o} + \theta_{2o}) = -\frac{\left(M_1 L_{c1y} + M_2 L_1\right)\cos(\theta_{1o}) + M_1 L_{c1x}\sin(\theta_{1o})}{M_2 L_{c2}} \tag{2}$$

$$M_2 g L_{c2}\cos(\theta_{1o} + \theta_{2o}) = T_{eq} \tag{3}$$

From Equation 2, given a particular θ_{1o}, the corresponding θ_{2o} can be calculated. This equation gives the family of equilibrium points around which the leg can be regulated. Equation 3 gives the equilibrium torque, T_{eq},that is needed to be supplied by the actuator. Since the system is to be controlled in a standing position and not tracking, linear equations of motion about an equilibrium point are needed. Hence, linearizing Equation 1 about (θ_{1o}, θ_{2o}, T_{eq}) gives

$$\begin{bmatrix} h_{11} & h_{12} \\ h_{21} & h_{22} \end{bmatrix}\begin{bmatrix} \left(\ddot{\theta}_1 - \ddot{\theta}_{10}\right) \\ \left(\ddot{\theta}_2 - \ddot{\theta}_{20}\right) \end{bmatrix} + \begin{bmatrix} g_1 \\ g_2 \end{bmatrix}\begin{bmatrix} \left(\theta_1 - \theta_{10}\right) \\ \left(\theta_2 - \theta_{20}\right) \end{bmatrix} = \begin{bmatrix} t_1 \\ t_2 \end{bmatrix} \tag{4}$$

where:

$$h_{11} = H_{11}(\theta_{20}),\quad h_{12} = H_{12}(\theta_{20})$$

$$h_{21} = h_{12},\quad h_{22} = H_{22}$$

$$g_1 = M_1 g\left[-L_{cly}\sin(\theta_{10}) + L_{clx}\cos(\theta_{10})\right] - M_2 g\left[L_1\sin(\theta_{10}) + L_{c2}\sin(\theta_{10} + \theta_{20})\right]$$

$$g_2 = -M_2 g L_{c2}\sin(\theta_{10} + \theta_{20})$$

$$t_1 = 0,\quad t_2 = T - T_{eq}$$

This linear equation can be put into familiar state space

$$\dot{x} = Ax + Bu,\quad y = Cx \tag{5}$$

where:

$$x_1 = \theta_1 - \theta_{1o},\quad x_2 = \theta_2 - \theta_{2o},\quad x_3 = \dot{\theta}_1,\quad x_4 = \dot{\theta}_2,\quad u = t_2$$

$$A = \begin{bmatrix} 0 & 0 & 1 & 0 \\ 0 & 0 & 0 & 1 \\ \dfrac{h_{22}g_{11} - h_{12}g_{12}}{\Delta} & \dfrac{h_{22}g_{12} - h_{12}g_{12}}{\Delta} & 0 & 0 \\ \dfrac{h_{11}g_{12} - h_{12}g_{11}}{\Delta} & \dfrac{h_{11}g_{12} - h_{12}g_{12}}{\Delta} & 0 & 0 \end{bmatrix}$$

$$B = \begin{bmatrix} 0 \\ 0 \\ -\dfrac{h_{12}}{\Delta} \\ \dfrac{h_{11}}{\Delta} \end{bmatrix},\quad C = \begin{bmatrix} 1 & 0 & 0 & 0 \\ 0 & 1 & 0 & 0 \end{bmatrix},$$

$$\Delta = h_{11}h_{22} - h_{12}^2$$

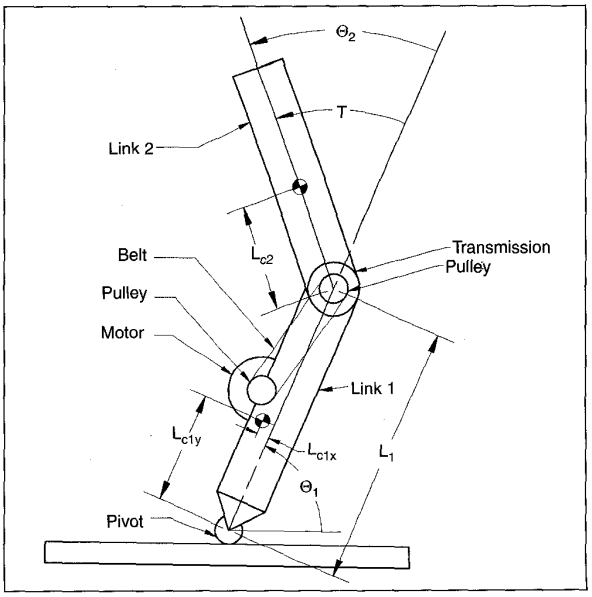

Fig. 3. The schematic model of the under-actuated leg.

Formulating the problem in this form allows investigation into how the physical parameters affect the system. In designing such a system one must know the conditions under which the system is controllable and observable. It can be shown that the system is observable at all points characterized by Equations 2 and 3. On the other hand, it can be determined that the system is always controllable iff

$$h_{11}g_{12} - h_{12}g_{11} \neq 0 \tag{6}$$

Thus the system is always controllable as long as the physical parameters are chosen such that the above condition is satisfied. The linear system given by Equation 5 as discussed before has one input (u) and two outputs (x_1 and x_2). Thus there are two transfer functions of interest:

$$G_1 = \frac{x_1}{u} = \frac{\left(s^2 - \frac{g_{12}}{h_{12}}\right)}{s^4 - \left(A(3,1) + A(4,1)\right)s^2 + \det(A)} \tag{7}$$

$$G_2 = \frac{x_2}{u} = \frac{\left(s^2 - \frac{g_{11}}{h_{11}}\right)}{s^4 - \left(A(3,1) + A(4,1)\right)s^2 + \det(A)} \tag{8}$$

Note that the dependence of transfer functions on s is not denoted throughout this article. Both transfer functions have two zeros and four poles. Since the numerators and denominators have non-odd powers of s, the poles and zeros will be symmetric about the imaginary axis. This fact makes the transfer functions unstable and non-minimum-phase, which can be affirmed from the physics of the system. Moreover, this imposes severe limitations on the closed-loop system bandwidth in rejecting disturbances and robustness in modeling error (parameter uncertainties). Since the physical parameters of a walking machine change (e.g. when a load is picked up), an adaptive control law should be implemented to adjust to the change in parameters. For a detailed analysis of these limitations consult [4,5].

Controller Design

The μ-synthesis approach was used to design the controller for the under-actuated leg. This approach allows performance objectives to be achieved in the presence of modeling uncertainty, which is an important consideration in this system. For further information on this technique consult [6].

Fig. 4 shows the interconnection structure used in the design procedure. The solid blocks represent the nominal linear model of the system represented by Equation 4. The weighting functions W_{p1}, W_{p2}, W_{p3} and the norm bounded stable transfer functions Δ_1 and Δ_2 are used to model plant uncertainty. The stable transfer functions Δ_1 and Δ_2 are assumed to be unknown except for the norm condition $\|\Delta_{1,2}\|_\infty < 1$. The frequency-dependent weighting functions W_1 through W_7 are used to define performance objectives which are described in detail below. These fictitious weighting functions are used in the controller design only and are not implemented in the actual closed-loop system. Only the controller K is actually implemented on the physical system. K is chosen from the set of 2-input, 1-output, real rational matrix functions which internally stabilize the closed-loop system. Fig. 5 represents a 4-input, 5-output transfer matrix $T(\Delta_1, \Delta_2, K)$ where the four inputs are D{2} and N{2}, and the five outputs are E{2}, u_{pen}, $\dot{u}_{pen}$, and $\dot{\Theta}_{pen}$. These are the signals used to define the performance objective. The goal of the controller design technique is to perform the following optimization:

$$\max_{\Delta_1,\Delta_2}\left[\min_{K}\left\|T(\Delta_1,\Delta_2,K)\right\|_\infty\right] \tag{9}$$

The choice of weighting functions will be discussed in detail below. Details are given in the experimental results section.

The block designated as W_{p1} is used to model the uncertainty in the actual torque applied to the system as compared to output of the controller. In this system, there is a belt-and-pulley system which is used to transfer power from the motor to the transmission. The belt-and-pulley system add extra dynamics to the output of the actuator. This weighting function allows for this extra dynamics to effect the controller design process.

The blocks designated as W_{p2} and W_{p3} are used to model the uncertainty in the physical parameters. A multiplicative model for uncertainty was used. The uncertainties in the individual parameters are all lumped together. Thus the uncertainty is only in the individual entries of the matrix A.

The block designated as W_1 is used to penalize the output from the controller. Since this is a physical system, there is a limit to the amount of torque that can be produced from the motor. This block incorporates the saturation of the actuator in the design process such that $\|W_1\|_\infty \leq \frac{1}{saturation}$.

The block designated as W_2 is used to penalize the derivative of the output signal from the controller. This penalty allows the designer control over the rate at which the controller output can change.

The block designated as W_3 is used to characterize the disturbance torques the system will experience during operation. The large-magnitude weighting functions correspond to large-magnitude disturbances.

The block designated as W_4 is used to orient the disturbance torques so they affect the system properly. W_4 was chosen as below.

$$W_4 = \begin{bmatrix} h_{11} & h_{12} \\ h_{21} & h_{22} \end{bmatrix}^{-1} \begin{bmatrix} 1 & -1 \\ 0 & 1 \end{bmatrix} \tag{10}$$

The block designated as W_5 is used to penalize the angular velocity of the second link. Penalizing $\dot{\theta}_2$ indirectly decreases the maximum excursion θ_2 undergoes. The larger the penalty, the slower link 2 will move when it leaves the equilibrium point.

The block designated as W_6 is used to set the performance objective. By adjusting the magnitude of this weighting function, the tracking error in angles can be specified. For example, if the weighting function for θ_1 was set to 100 at DC, then the controller would be designed to give 1% tracking at DC.

The block designated as W_7 is used to model the corruption of each measurement with sensor noise. The noise was assumed to be additive.

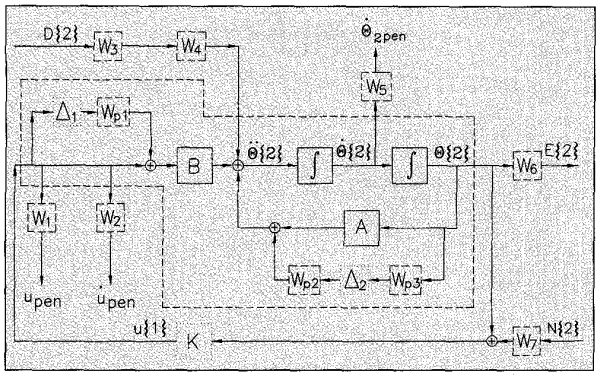

Fig. 4. The controller architecture.

This interconnection structure was used to design a controller iteratively using the μ-Analysis and Synthesis Toolbox for MATLAB.

Experimental Results

A physical system of the leg was built at UC Berkeley (Fig. 5). The physical parameters for the actual leg based on the model are as follows:

$L_{c1y} = 0.298\text{m}$, $L_{c1x} = 0.008\text{m}$, $L_{c2} = 0.304\text{m}$, $L_1 = 0.508\text{m}$, $M_1 = 17.007\text{kg}$, $M_2 = 8.174\text{kg}$, $I_1 = 0.559\text{kgm}^2$, $I_2 = 0.390\text{kgm}^2$, $I_m = 0.0020\text{kgm}^2$, and n = 60.

Since the H_∞ optimal control design was used, a set of weighting functions as described above had to be chosen. The weighting functions are:

$$W_{p1} = \frac{5s+74}{s+1472}, \quad W_{p2} = \begin{bmatrix} 4\% & 4\% & 0 & 0 \\ 0 & 0 & 4\% & 4\% \end{bmatrix},$$

$$W_{p3}^T = \begin{bmatrix} 1 & 0 & 1 & 0 \\ 0 & 1 & 0 & 1 \end{bmatrix}$$

$$W_1 = \frac{4s+14.6}{s+194}, \quad W_2 = \frac{5s}{s+5},$$

$$W_3 = \begin{bmatrix} \frac{0.001s+0.5}{50s+1} & 0 \\ 0 & \frac{0.001s+0.5}{10s+1} \end{bmatrix}$$

$$W_5 = \frac{5s+63.2}{s\_253}, \quad W_6 = \begin{bmatrix} \frac{0.5s+8.66}{s+0.11} & 0 \\ 0 & \frac{0.5s+0.867}{s+0.043} \end{bmatrix},$$

$$W_7 = \begin{bmatrix} 0.000125 & 0 \\ 0 & 0.000025 \end{bmatrix}$$

W_{p1} was chosen such that at low frequencies there is only 5% uncertainty in the torque delivered to the transmission and 100% at high frequencies where the crossover frequency was set at 300 rad/sec. The crossover was set here since 375 rad/sec is the frequency that excites the first mode of the belt. Thus, higher order dynamics of the belt enter close to this frequency and should be noted.

W_{p2} and W_{p3} were chosen such that there is a 4% multiplicative uncertainty in A(3,1), A(3,2), A(4,1), and A(4,2).

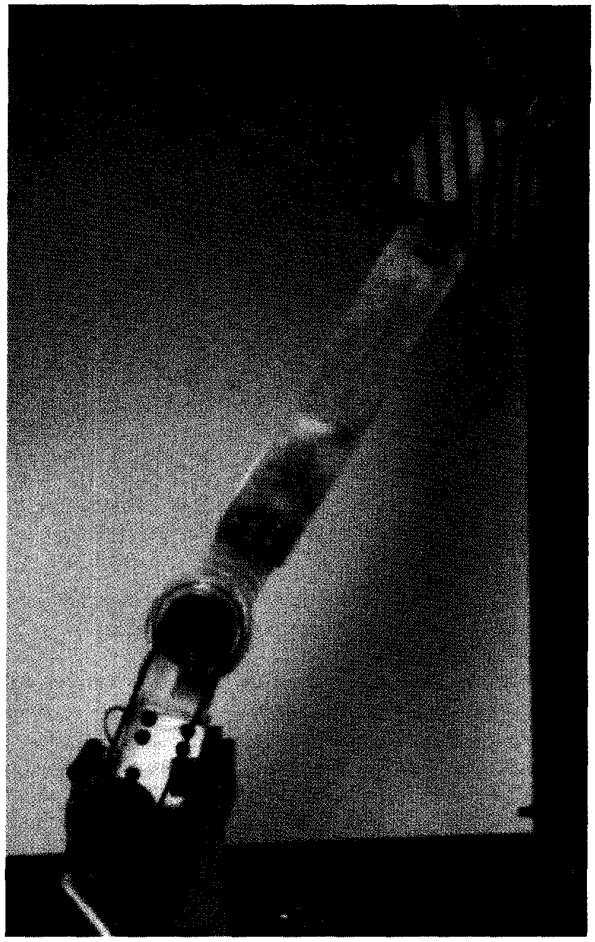

Fig. 5. The experimental under-actuated leg at the University of California, Berkeley.

W_1 was chosen such that at low frequencies the controller output is limited to 13.3Nm, and at high frequencies the output is limited to .25Nm. These bounds were chosen such that at low frequencies the command input to the servoamplifier would remain in its linear range. At high frequencies which would typically occur if the system went unstable, the gain was chosen so no damage would occur to the system. The crossover frequency was set to 50 rad/sec, well above normal operation.

W_2 was chosen such that at low frequencies it would be a differentiator with a gain of 5 and level off at 5 rad/sec.

W_3 was chosen such that at low frequencies the system could reject a disturbance torque of 0.5Nm on both links. The cutoff frequencies for both were set to 0.01 rad/sec.

W_5 was chosen such that at low frequencies $\dot{\theta}_2$ is limited to 4 rad/sec, and at high frequencies is limited to 0.2 rad/sec. The crossover frequency was set to 50 rad/sec.

W_6 was chosen such that at low frequencies there is only 1.25% error in tracking in θ_1 and 5% error in tracking in θ_2. The crossover frequencies were set to 10 rad/sec and 1 rad/sec for θ_1 and θ_2, respectively. At higher frequencies the performance specifications were relaxed to 200% error.

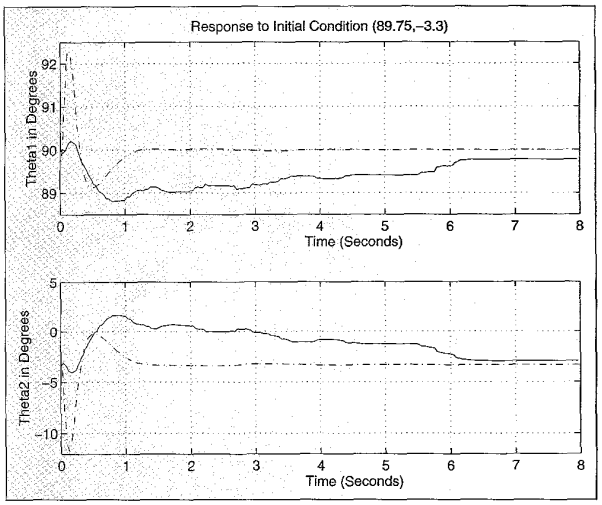

Fig. 6. Simulated (dashed) and actual (solid) system response.

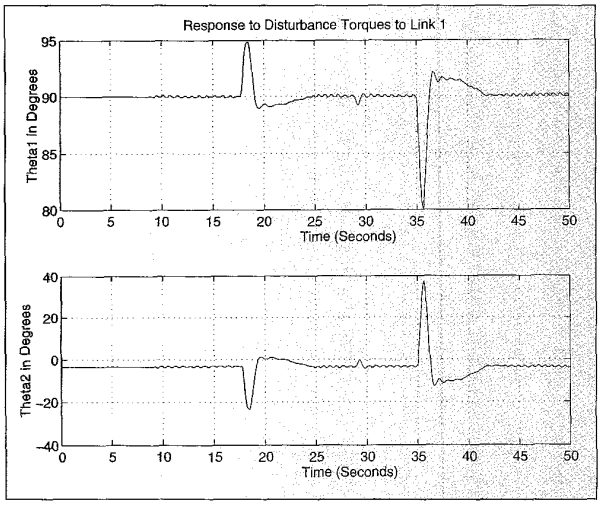

Fig. 7. Effect of disturbance torque on Link 1.

W_7 was chosen to be the smallest unit of measurement for both devices. Since both devices were high-precision, low-noise encoders, this bound is reasonable.

With these weighting functions, an 18th-order controller was developed which achieved a μ of 0.966. Thus, robust performance and robust stability are guaranteed on the linear plant.

Fig. 6 shows the real-time response of the system subject to the controller designed above. Both a simulated (dashed) and real (solid) response are shown. In the actual system, the initial deviations from equilibrium are smaller. However, the secondary deviations are larger. This effect occurs since there is friction in the system, which is slowing down the system. Another interesting feature is that the time responses for θ_1 and θ_2 seem symmetrical. This symmetry can be seen from Equation 4. The system must satisfy this equation to be in equilibrium. Thus, this equation constrains the angles such that if θ_1 moves counterclockwise, θ_2 must move clockwise to keep the center of mass over the pivot point. As shown, steady-state error exists in both angles. θ_1 settles to 89.78°, and θ_2 settles to -3.15°. Both of these deviations are within the performance specifications from the W_6 weighting function.

The next experiment was to test the system's robustness to disturbances. Fig. 7 shows the response of the system to three disturbance torques to Link 1. In this system, disturbance rejection is defined in a slightly different way. In conventional practice, controllers are designed such that disturbances have no effect on the output. However, since this system is under-actuated, the center of mass must move to counteract any disturbance torques imposed on it. Thus, the angles will change from the desired value in order to maintain stability. The first disturbance is a torque in the counterclockwise direction with a magnitude of approximately 0.2Nm. It is applied at approximately 17 seconds and then released at 18 seconds. The system then returns to equilibrium in 7 seconds. As noted before, θ_2 moves in the opposite direction of θ_1 such that the center of mass of the system remains above the pivot point. A small disturbance torque is applied at 29 seconds. A torque of approximately 0.5Nm was applied in the clockwise direction at 35 seconds, which was the maximum disturbance torque included in the design. The system recovered in approximately 7 seconds again. The same behavior was observed when disturbances were imposed on Link 2.

Conclusion

We propose using two under-actuated robotic systems as two legs of a walking machine. Since the ankle joints of both legs have no actuation, the walking machine remains upright only when it is balanced via a computer-controller. The design of a stabilizing controller for one under-actuated leg, using a μ-synthesis approach, is explained in detail. The system at the equilibrium can be represented by a non-minimum phase system. The right half plane zero severely limits the achievable closed-loop bandwidth and robustness in modeling errors.

Appendix: Nomenclature

L_{c1y}: Distance to center of mass of Link 1 along the center line

L_{c1x}: Distance to center of mass of Link 1 orthogonal to center line

L_{c2}: Distance to center of mass of Link 2 along the center line

L_1: Length of Link 1

M_1: Mass of Link 1

M_2: Mass of Link 2

I_1: Moment of inertia of Link 1 about center of mass

I_2: Moment of inertia of Link 2 about center of mass

I_m: Moment of inertia of transmission, pulley, and belt

n: Transmission reduction ratio

H: 2 x 2 inertia matrix

V: 2 x 1 Coriolis vector

G: 2 x 1 gravity vector

h: 2 x 2 linearized inertia matrix at the operating point

g: 2 x 1 linearized gravity vector at the operating point

θ_1: Angle of Link 1 relative to horizontal (+ CCW)

θ_2: Angle of Link 2 relative to Link 1 (+ CCW)

θ_{10}: Equilibrium angle for Link 1 relative to horizontal

θ_{20}: Equilibrium angle for Link 2 relative to Link 1

T: Torque provided for transmission (+ CCW)

T_{eq}: Equilibrium torque

τ: 2 x 1 input torque vector

t: 2 x 1 input torque vector for linearized equations of the motion
x: 4 x 1 vector of states
u: Input to linear system
y: 2 x 1 output vector of linear system
$D\{2\}$: 2 x 1 disturbance torque vector
$E\{2\}$: 2 x 1 error vector
$N\{2\}$: 2 x 1 noise vector
$\Theta\{2\}$: 2 x 1 joint angle vector
$K(s)$: Controller (1 x 2 transfer function matrix)

References

[1] S.A. Bortoff and W.M. Spong, "Psuedolinearization of the Acrobat Using Spline Functions," *Proceedings of the 31st IEEE Conference on Decision and Control*, New York, New York: IEEE 1992.

[2] H. Kazerooni and H. Mahoney, "Dynamics and Control of Robotic Systems Worn by Humans," *ASME Journal of Dynamic Systems, Measurement, and Control*, vol. 133, no. 3, September 1991.

[3] H. Kazerooni and J. Guo, "Human Extenders," *ASME Journal of Dynamic Systems, Measurements, and Control*, vol. 115, no. 2(B), June 1993.

[4] J.C. Doyle, B.A. Francis, and A.R. Tannendanm, *Feedback Control Theory*, New York, NY: Macmillan Publishing Company, 1992.

[5] J.S. Freudenberg and D.P. Looze, "Lecture Notes in Control and Information Sciences," Berlin, Germany: Springer-Verlag Publishing, 1988.

[6] Gary J. Balas, J.C. Doyle, Keither Glover, Andrew Packard, and Roy Smith, *Mu-Analysis and Synthesis Toolbox*, Mathworks Inc., 1994.

Satinder Pannu received a B.S. degree from the University of California at Berkeley in 1992. From 1992 to 1994, he was a graduate student at the Human Engineering Laboratory. He is currently working on his Ph.D. at the University of California at Berkeley in the area of adaptive compensation for disk drives.

H. Kazerooni received an M.S. degree from the University of Wisconsin at Madison in 1980, and M.S.M.E. and Sc.D. degrees in mechanical engineering from MIT in 1982 and 1984, respectively. From 1984 to 1985, he was a post-doctoral fellow at the MIT Laboratory for Manufacturing and Productivity. From 1985 to 1990 he served as an assistant professor and then associate professor at the University of Minnesota in Minneapolis, where he held the McKnight-Land Grant Professorship. He is currently a professor in the Mechanical Engineering Department and director of the Human Engineering Laboratory (HEL) at the University of California at Berkeley. His research areas involve control theory and applications, mechatronics design, bioengineering, human-machine systems, and automated manufacturing.

Gregory Becker is currently a research scientist at INRIA, working on applications of linear matrix inequalities to advanced control system design. He attended UC Berkeley from 1985-1993, earning B.S., M.S., and Ph.D. degrees in mechanical engineering. He is a registered professional engineer in the state of California. His technical interests are robust control and control of parameter-dependent systems.

Andrew Packard is an associate professor in mechanical engineering at the University of California, Berkeley. Before that, he was a research fellow at Caltech in 1988, and an assistant professor in electrical engineering at University of California at Santa Barbara in 1989. He earned his Ph.D. in mechanical engineering at UC Berkeley in January 1988. His technical interests are control of parameter-dependent systems, robust control, and user-interfaces for control system design and real-time implementation.

Sampled Data

An Analytic Study of the Least Publishable Increment

Abstract

This paper presents an analytic study of the least publishable increment (LPI). The LPI is defined as the smallest acceptable difference between two publishable papers. Two metrics for the LPI are derived. The first metric is based on a generalized distance measure derived from the famous Hausdorf metric and is used to differentiate between papers on similar topics by different authors. The second metric describes a distance measure for papers from the same author.

Further studies using cross-journal and conference proceedings relations are also discussed. We outline a simple strategy for maximal publication based on these distance measures. An illustrative example of the maximal publication scheme is shown, and its correlation to actual publication scheme is also given.

We present proof that maximal publication based on the LIP is an optimal approach for junior faculty members attempting to get tenure.

—Anonymous, from the Editor's email